PDE Based Methods for Finding Global Minima

Selim Esedoglu

Based on joint works with:

Tony Chan, Mila Nikolova;

Xavier Bresson, Stan Osher, Pierre Vandergheynst, and J. P. Thiran.

Based mainly on the works:

1. Chan, T. F.; Esedoglu, S. *Aspects of total variation regularized L^1 function approximation.* UCLA CAM Report 04-07, **February 2004**. SIAM J. Appl. Math **65**:5 (2005), pp. 1817 - 1837.
2. Chan, T. F.; Esedoglu. S.; Nikolova, M. *Algorithms for finding global minimizers of denoising and segmentation models.* UCLA CAM Report 04-54, **September 2004**. SIAM J. Appl. Math. **66** (2006), pp. 1632 - 1648.
3. Bresson, X.; Esedoglu, S.; Vandergheynst, P.; Thiran, J. P.; Osher, S. *Fast global minimization of the active contours/ snake model.* UCLA CAM Report 05-04, **January 2005**. J. Math. Imaging and Vision. **28**:2 (2007), pp. 151 - 167.

Outline

1. Rudin-Osher-Fatemi with L^1 Fidelity.
2. Contrast invariance.
3. Exact solutions.
4. Application to Image Decomposition.
5. Application to Shape Denoising.
6. Application to Image Segmentation.
7. Convex duality based numerical optimization.
8. Fast solution of the dual problem.

Standard Total Variation Model

- Rudin, Osher, and Fatemi (1992):

$$E_2(u) = \int |\nabla u| + \lambda(f - u)^2 \, dx$$

- Preserves sharp edges.
- Many advantages over Perona-Malik:
  - Strictly convex functional: Existence, uniqueness of solutions.
  - Continuous dependence on data (i.e. f), and parameters (i.e. λ).
  - Only one parameter to be chosen by user: λ
- Still some difficulties:
  - Non-differentiable.
  - Naïve numerical methods slow to converge.
- Intimately related to: Piecewise constant Mumford-Shah.

Total Variation: Basic Facts

- To define total variation for possibly discontinuous functions:
- Given a vector $x \in \mathbb{R}^n$, we can write:

$$|x| = \max_{|y| \leq 1} x \cdot y$$

- Apply this to

$$\int |\nabla u| dx = \int \max_{|g| \leq 1} g \cdot \nabla u \; dx$$

- When $u(x)$ is smooth, can take $g(x)$ to be smooth and compactly supported, and move "max" outside:

$$\int |\nabla u| dx = \sup_{\substack{|g(x)| \leq 1 \\ g \in C_c^1}} \int g \cdot \nabla u \, dx$$

Total Variation: Basic Facts

- Integrate by parts:

$$\int |\nabla u| dx = \sup_{\substack{|g(x)| \leq 1 \\ g \in C_c^1}} \int u \, \nabla \cdot g \, dx$$

- Right hand side can be finite even for discontinuous u.
- It is taken to be the definition of total variation:

$$\boxed{\int |\nabla u| = \sup_{\substack{|g(x)| \leq 1 \\ g \in C_c^1}} \int u \, \nabla \cdot g \, dx}$$

Total Variation: Basic Facts

- Example:

$$u(x) = \mathbf{1}_{\Sigma}(x)$$

where Σ is a compact set with smooth boundary $\partial\Sigma$.

- First of all,

$$\int u \, \nabla \cdot g \, dx = \int_{\Sigma} \nabla \cdot g \, dx = \int_{\partial\Sigma} g \cdot n \, d\sigma \leq \int_{\partial\Sigma} d\sigma = \mathrm{Length}(\partial\Sigma)$$

- Second: There exists a vector field $\psi(x)$ s.t.
  1. ψ is smooth, compactly supported,
  2. $|\psi(x)| \leq 1$ for all x,
  3. $\psi(x) = n(x)$ for all $x \in \partial\Sigma$.
- We have:

$$\int u \, \nabla \cdot g \, dx = \int_{\partial\Sigma} n \cdot n \, d\sigma = \mathrm{Length}(\partial\Sigma)$$

Total Variation: Basic Facts

- Hence, we see that

$$\int |\nabla \mathbf{1}_{\Sigma}(x)| = \mathrm{Length}(\partial\Sigma) \coloneqq \mathrm{Per}(\Sigma)$$

  when $\partial\Sigma$ is smooth.

- If $u(x)$ is piecewise constant:

$$u(x) = \sum_{j=1}^{N-1} (c_j - c_{j-1}) \mathbf{1}_{\Sigma_j}(x)$$

with $c_{j+1} > c_j > 0$, $\Sigma_j \subset \Sigma_{j+1}$, and $\partial\Sigma_j$ smooth for all j, then:

$$\int |\nabla u| = \sum_{j=1}^{N-1} (c_{j+1} - c_j)\mathrm{Per}(\Sigma_j) = \sum_{j=1}^{N-1} (c_{j+1} - c_j)\mathrm{Per}(\{x : u > c_j\})$$

Total Variation: Basic Facts

- Given any function $u \in L^1$, approximate by such piecewise constant functions.
- Use our formula.
- Pass to the limit.
- You get the co-area formula

$$\boxed{\int |\nabla u| = \int_{\mathbb{R}} \mathrm{Per}(\{x : u(x) > \mu\})\, d\mu}$$

Standard ROF Model: Caveats

- Contrast loss: Consider the given image

$$f(x) = \mathbf{1}_{B_R(0)}(x)$$

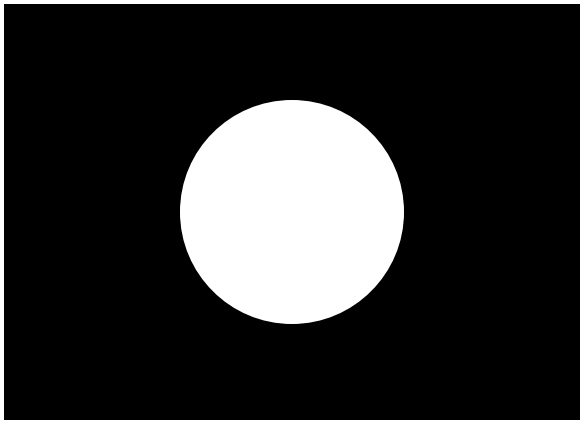

- Exact solution:

$$u = c(\lambda, R)\mathbf{1}_{B_R}(x)$$

where

$$\boxed{c(\lambda, R) = \max\left\{1 - \frac{1}{\lambda R}, 0\right\}}$$

Standard ROF Model: Caveats

- The image
$$f(x) = \mathbf{1}_{B_R(0)}(x)$$
is noise free.
- Boundary (edges) $\partial B_R(0)$ reconstructed exactly.
- However, there is contrast loss.
- QUESTION: What images are exactly preserved by the ROF model?
i.e. which images are treated as noise free?

ANSWER (Y. Meyer): The only image that the ROF model reconstructs exactly is

$$f(x) \equiv 0.$$

Standard ROF Model: Caveats

- Relaxed QUESTION: For which images of the form

$$f(x) = \mathbf{1}_\Omega(x)$$

does the ROF model reconstruct the shape boundary exactly:

$$u(x) = c(\lambda)\mathbf{1}_\Omega(x) \ ?$$

- Answer (Bellettine, Caselles, Novaga): ROF preserves the boundary of only very special shapes: Ω should be bounded and convex, with $C^{1,1}$ boundary, and satisfy an inequality of the form:

$$\boxed{\sup_{x\in\partial\Omega} \kappa(x) \leq \frac{\mathrm{Per}(\Omega)}{|\Omega|}}$$

ROF Model with L^1 Fidelity

$$E(u) = \int |\nabla u| + \lambda |f - u| \, dx$$

- Tiny perturbation of the original model.
- Useful advantages:
  - Contrast invariance.
  - Leaves many clean images invariant.
  - Leads to algorithms for finding global minima of

    Segmentation, and

    Denoising models.
- E_1 is convex, but not strictly so.

ROF Model with L^1 Fidelity

Theorem Let $D = \mathbb{R}^2$ and $f(x) = \mathbf{1}_\Omega(x)$, where Ω is a bounded domain with C^2 boundary $\partial\Omega$. There exists λ_* such that if $\lambda > \lambda_*$, then the unique minimizer of $E_1(\cdot, \lambda)$ is given by $u(x) \equiv f(x)$.

Proof: Let $\phi(x)$ be a vector field such that:

1. $\phi(x) \in C_c^1(\mathbb{R}^n)$,
2. $|\phi(x)| \leq 1$ for all x,
3. $\phi(x) = n(x)$ for all $x \in \partial\Omega$.

(i.e. extend the normal off of $\partial\Omega$).

ROF Model with L^1 Fidelity

Then, we have:

$$\int |\nabla f| = \int f \operatorname{div} \phi \; dx$$

and so:

$$\begin{aligned}
E_1(u,\lambda) &= \int |\nabla u| + \lambda \int |u-f|\,dx \\
&\geq \int u \operatorname{div} \phi \, dx + \lambda \int |u-f|\,dx \\
&= \int f \operatorname{div} \phi \, dx + \lambda \int |u-f|\,dx + \int (u-f) \operatorname{div} \phi \, dx \\
&\geq E_1(f,\lambda) + \Big(\lambda - \max_{x \in \mathbf{R}^N} |\operatorname{div} \phi(x)|\Big) \int |u-f|\,dx.
\end{aligned}$$

ROF Model with L^1 Fidelity

- UPSHOT:
  - There is no contrast loss.
  - Many clean images are preserved exactly (treated as noise free).

Shape Denoising

Problem Statement: Given a binary observed image $f(x)$, to find a denoised (regularized) version. A binary image can be represented as:

$$f(x) = \mathbf{1}_\Omega(x)$$

where Ω is some domain in D, with possibly very rough boundary.

Applications: There are many (Osher):

- Denoising of fax documents ($D \subset \mathbf{R}^2$).
- Fairing of surfaces in computer graphics ($D \subset \mathbf{R}^3$).
- Understanding important segmentation models, which are closely related: Mumfod-Shah and its variants.

Restriction of ROF to Binary Images

Take $f(x) = \mathbf{1}_\Omega(x)$ and restrict minimization to set of binary images:

$$\min_{\substack{\Sigma \subset D \\ u(x) = \mathbf{1}_\Sigma(x)}} \int_D |\nabla u| + \lambda \int_D \Big(u(x) - \mathbf{1}_\Omega(x) \Big)^2 \, dx$$

It is of course equivalent to the following geometry problem: Given a set $\Omega \subset D$,

$$\boxed{\min_{\Sigma \subset D} \mathrm{Per}(\Sigma) + \lambda |\Sigma \triangle \Omega|}$$

where we use the following notation:

- $S_1 \triangle S_2$ denotes the symmetric difference of the sets S_1 and S_2:

$$S_1 \triangle S_2 = (S_1 \setminus S_2) \cup (S_2 \setminus S_1) \, .$$

- $|\cdot|$ denotes area in 2D, volume in 3D.

Considered using level sets: Osher & Kang, Osher & Vese, etc.

Geometry Problem

$$\boxed{\min_{\Sigma \subset D} \mathrm{Per}(\Sigma) + \lambda |\Sigma \triangle \Omega|}$$

- This is a non-convex optimization problem, since the set of binary functions is non-convex.
- The global minimizer is not unique in general.
- In general, in addition to more than one global minimizer, there are also local minimizers.

Local Minima

Terzopoulos snakes, standard level sets (with reinitialization), etc.

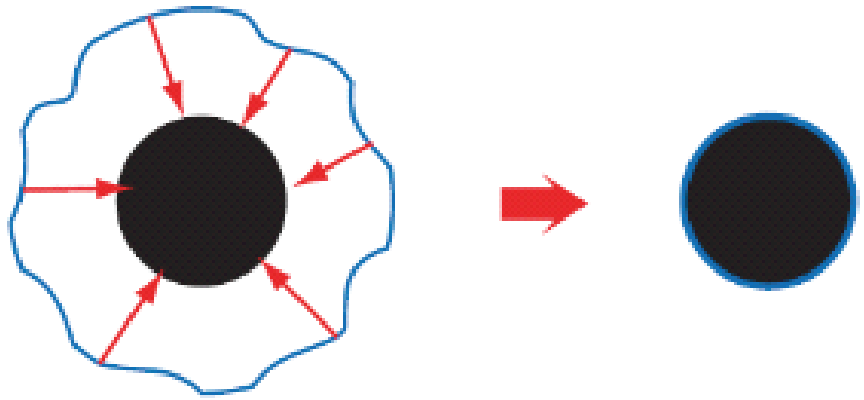

Other types of local minima:

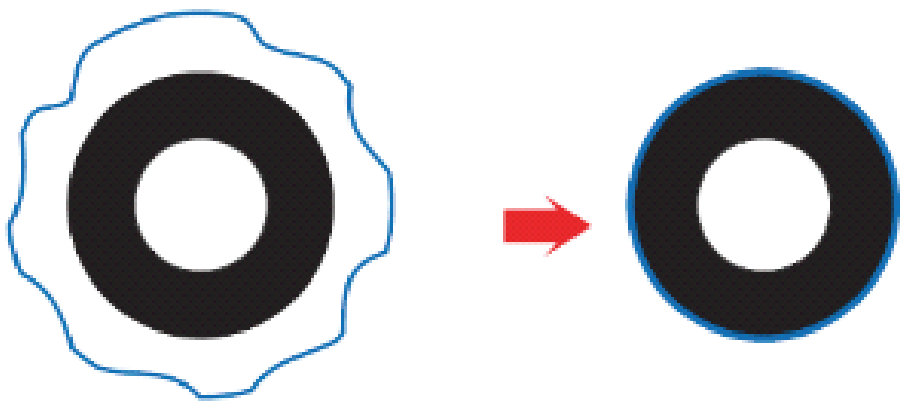

It is easy to verify rigorously that these scenarios do arise.

Solution via TVL^1:

Claim: To find a solution (i.e. a global minimizer) $u(x)$ of the non-convex variational problem

$$\boxed{\min_{\Sigma \subset D} \mathrm{Per}(\Sigma) + \lambda |\Sigma \triangle \Omega|}$$

it is sufficient to carry out the following steps:

1. Find any minimizer of the **convex** energy

$$E_1(u) := \int_D |\nabla u| + \lambda \int_D \left| u(x) - \mathbf{1}_\Omega(x) \right| dx.$$

   Call the solution found $v(x)$.

2. Let $\Sigma = \{x \in D : v(x) > \mu\}$ for some $\mu \in (0, 1)$.

Then Σ is a global minimizer of the original non-convex problem for almost every choice of μ.

Solution via TVL^1

Proof is based on the following formula for the energy E_1:

$$E_1(u) = \int_{-\infty}^{\infty} \mathrm{Per}\left(\{x : u(x) > \mu\}\right) + \lambda \Big| \{x : u(x) > \mu\} \triangle \{x : f(x) > \mu\} \Big| \, d\mu$$

This entails two ingredients:

- Coarea formula:

$$\int_{\mathbf{R}^N} |\nabla u| = \int_{\mathbf{R}} \mathrm{Per}(\{x : u(x) > \mu\}) \, d\mu.$$

- "Layer Cake" theorem:

$$\int_{\mathbf{R}^N} \Big| u(x) - f(x) \Big| \, dx = \int_{\mathbf{R}} \Big| \{x : u(x) > \mu\} \triangle \{x : f(x) > \mu\} \Big| \, d\mu$$

Solution via TVL^1

Theorem: Let the observed image $f(x)$ be the characteristic function of a bounded domain $\Omega \subset \mathbf{R}^N$. Fix a $\lambda \geq 0$, and let $u_\lambda(x) \in M(\lambda)$ be any minimizer of $E_1(\cdot, \lambda)$. Then, for almost every $\mu \in [0, 1]$ we have that the binary function

$$\mathbf{1}_{\{x : u_\lambda(x) > \mu\}}(x)$$

is also a minimizer of $E_1(\cdot, \lambda)$.

Proof: When $f(x) = \mathbf{1}_\Omega(x)$, formula of the previous proposition becomes:

$$E_1(u, \lambda) = \int_0^1 \mathrm{Per}\Big(\underbrace{\{x : u(x) > \mu\}}_{:=\Sigma(\mu)}\Big) + \lambda \Big| \underbrace{\{x : u(x) > \mu\}}_{:=\Sigma(\mu)} \triangle \Omega \Big| \, d\mu$$

Setting $\Sigma(\mu) := \{x : u(x) > \mu\}$, this suggests that we consider for each level set of $u(x)$ our geometry problem:

$$\boxed{\min_{\Sigma \subset \mathbf{R}^N} \mathrm{Per}(\Sigma) + \lambda |\Sigma \triangle \Omega|}$$

Solution via TVL^1

Let $\Sigma_* \subset \mathbf{R}^N$ be a minimizer of the geometry problem. Then,

$$\mathrm{Per}\big(\Sigma(\mu)\big) + \lambda\big|\Sigma(\mu) \triangle \Omega\big| \geq \mathrm{Per}(\Sigma_*) + \lambda\big|\Sigma_* \triangle \Omega\big|$$

for all μ. This implies:

$$E_1(u_\lambda(x), \lambda) \geq E_1(\mathbf{1}_{\Sigma_*}(x), \lambda)$$

which means that $\mathbf{1}_{\Sigma_*}(x)$ is also a minimizer of $E(\cdot, \lambda)$. Conversely, since $u_\lambda(x)$ is a minimizer, we must really have:

$$E_1(u_\lambda(x), \lambda) = E_1(\mathbf{1}_{\Sigma_*}(x), \lambda).$$

That leads to the conclusion:

$$\mathrm{Per}\big(\Sigma(\mu)\big) + \lambda\big|\Sigma(\mu) \triangle \Omega\big| = \mathrm{Per}(\Sigma_*) + \lambda\big|\Sigma_* \triangle \Omega\big| \text{ a.e. } \mu.$$

$\Rightarrow$ $\Sigma(\mu)$ is a minimizer of the geometry problem for a.e. $\mu \in (0, 1)$.

$\Rightarrow$ $\mathbf{1}_{\Sigma(\mu)}(x)$ is a minimizer of $E_1(\cdot, \lambda)$.

Previous Work

This idea of writing total variation based optimization problems in terms of super-level sets goes back (at least) to the works of G. Strang for problems in plasticity:

$$\min_{\int_D uf\,dx=1} \int_D |\nabla u|$$

It is shown that the minimizer is achieved at a characteristic function for the optimization problem above.

- Strang, G. *L^1 and L^∞ approximation of vector fields in the plane.* Nonlinear Partial Differential Equations in Applied Science (Tokyo, 1982), pp. 273 – 288. North-Holland Math. Stud. 81. North Holland, Amsterdam, 1983.

- Strang, G. *Maximal flow through a domain.* Mathematical Programming. **26**:2 (1983), pp. 123 – 143.

Example: Original binary image $f(x)$:

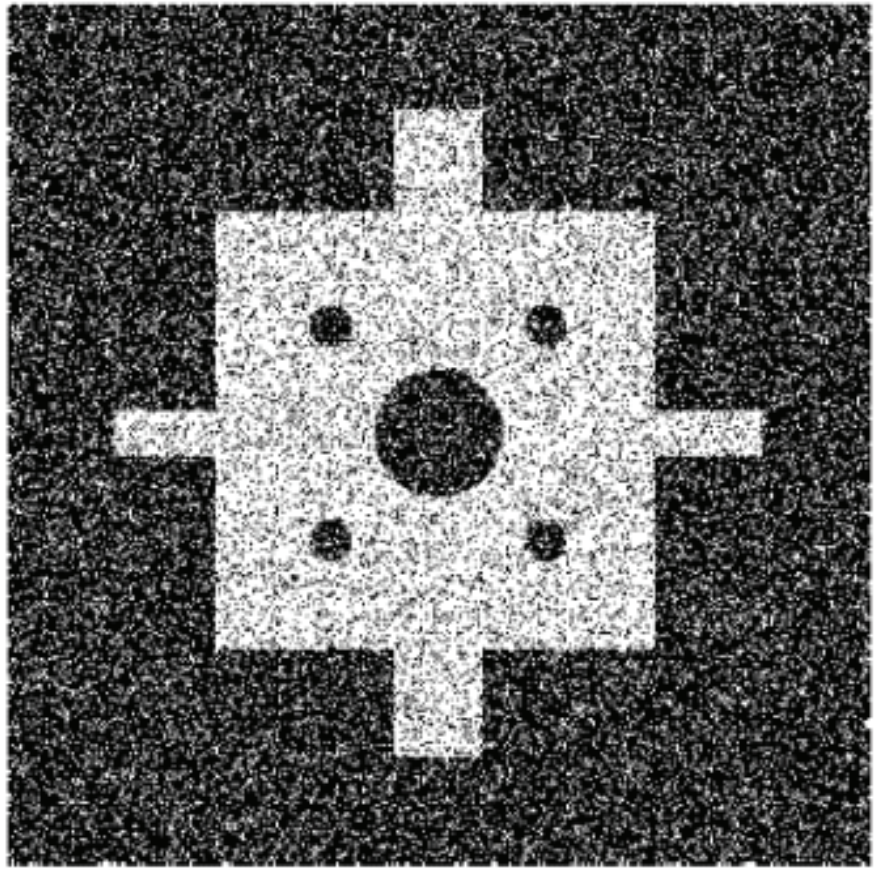

Minimizer of E_1 found:

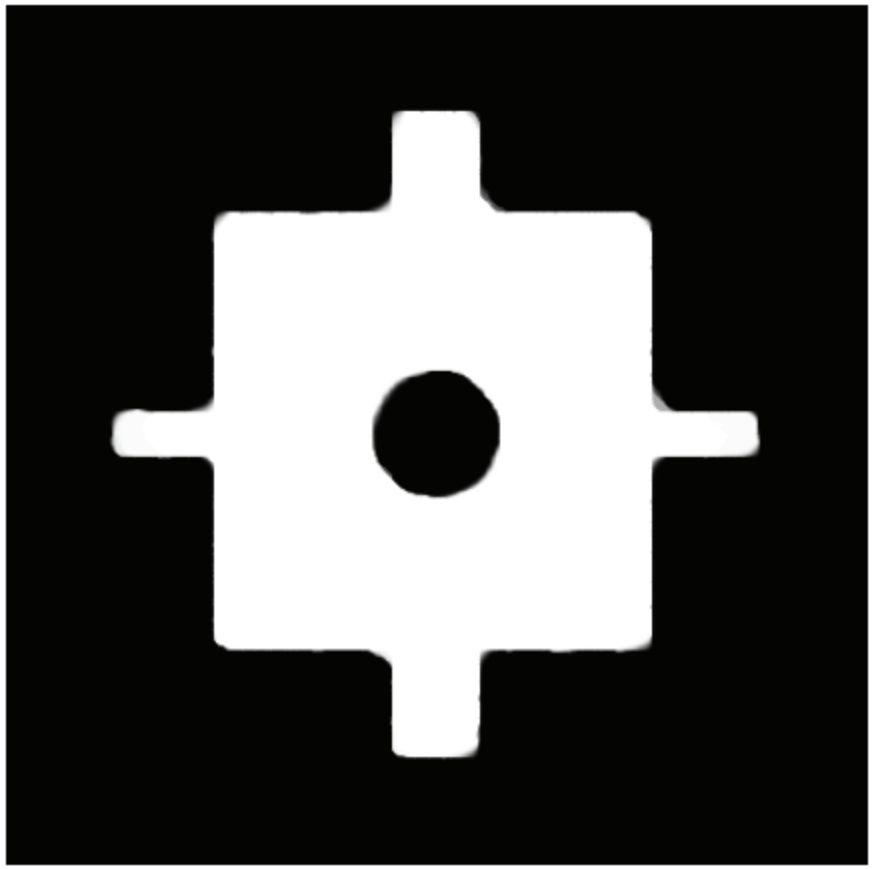

Intermediates, showing the evolution:

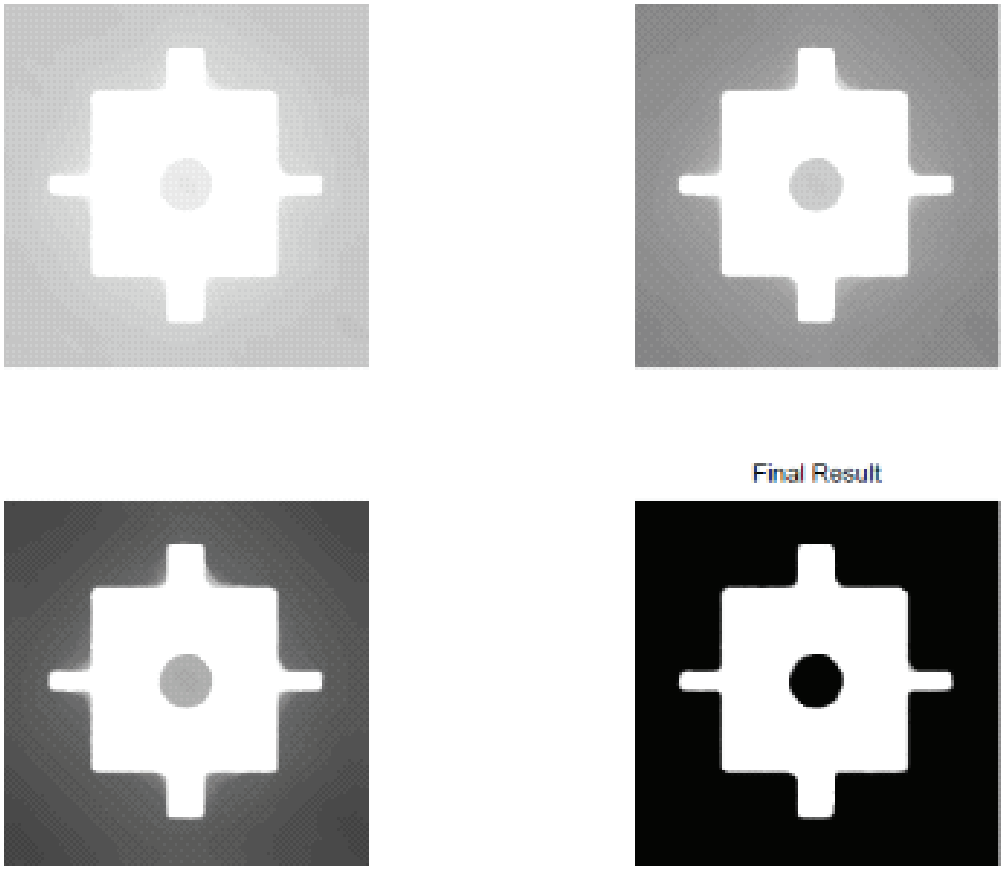

Histograms of the intermediates:

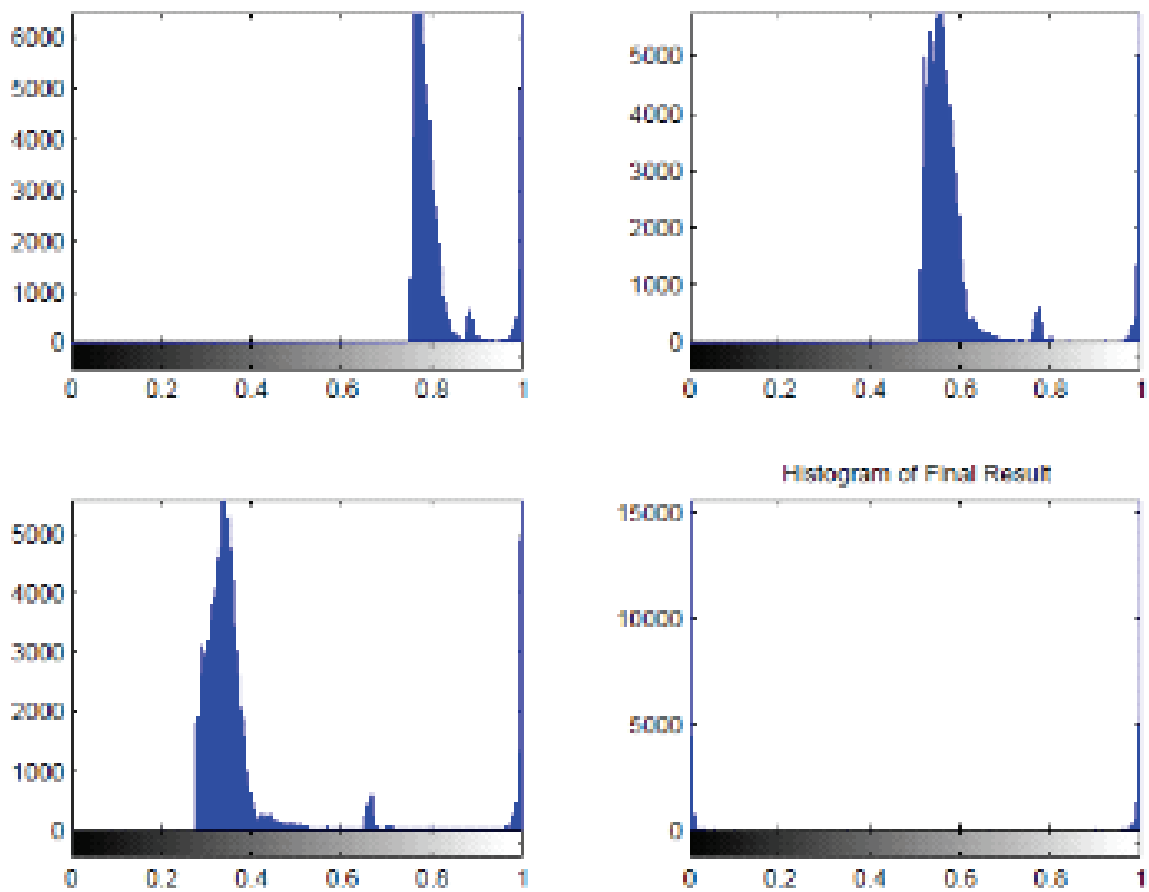

UPSHOT: Need to go through non-binary images to avoid getting stuck in local minimizers.

Application: Multiscale Decomposition

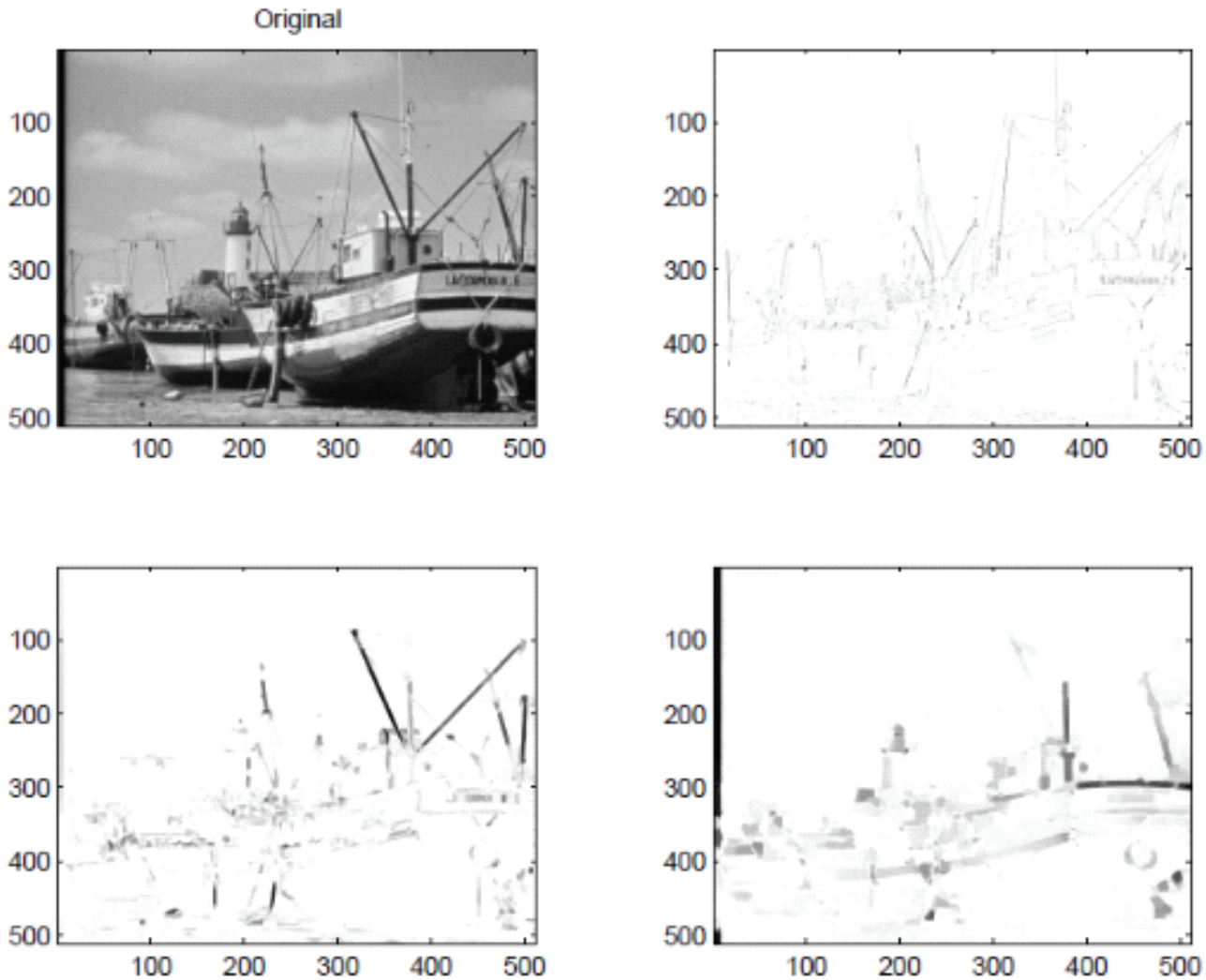

As in: E. Tadmor, S. Nezzar, L. Vese.

Application: Multiscale Decomposition

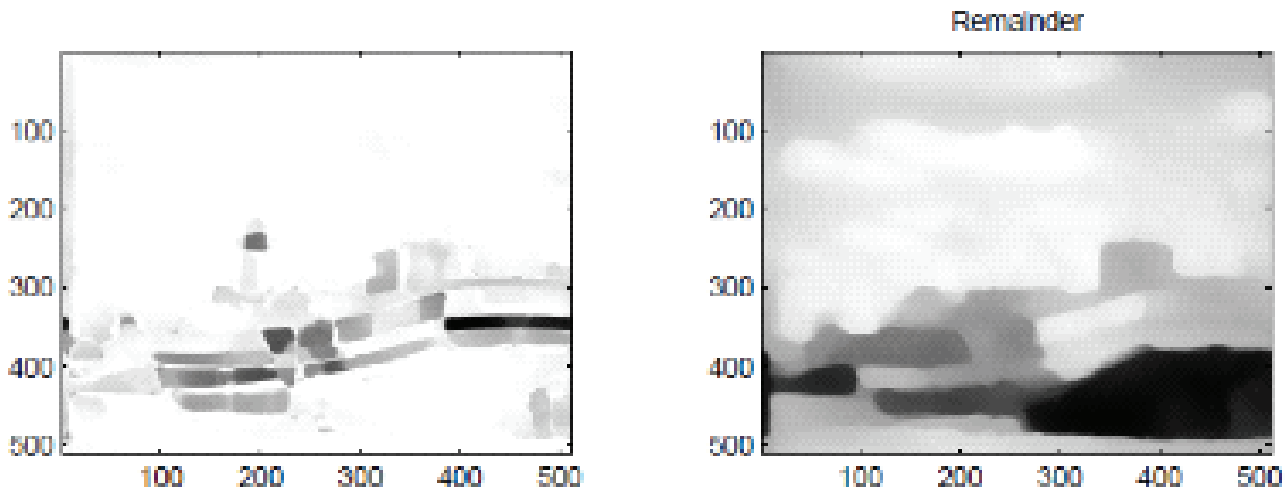

- Much cleaner decompositions than what's possible with standard ROF model.

- Many further results in this direction by Yin, Osher, Goldfarb, especially concerning cartoon – texture decomposition of images.

Generalization to P. C. Mumford-Shah

- Piecewise constant Mumford-Shah model of Chan & Vese:

$$\min_{\substack{c_1,c_2\in\mathbb{R}\\ \Sigma\subset D}} \mathrm{Per}(\Sigma) + \lambda \underbrace{\left\{ \int_\Sigma (c_1 - f)^2\,dx + \int_{D\setminus\Sigma} (c_2 - f)^2\,dx \right\}}_{=\int_D (u-f)^2\,dx}$$

- Best approximation of the image $f(x)$ among images that take only two values:

$$u(x) = c_1 \mathbf{1}_\Sigma(x) + c_2 \mathbf{1}_{D\setminus\Sigma}(x)$$

Generalization to P. C. Mumford-Shah

- **Our formulation:**

$$\min_{c_1,c_2\in\mathbb{R}} \min_{0\le u(x)\le 1} \int_D |\nabla u| + \lambda \int_D \left\{(c_1-f)^2-(c_2-f)^2\right\} u(x)\,dx.$$

Claim: If $(c_1, c_2, u(x))$ is a solution of above problem, then

$$\left(c_1, c_2, \mathbf{1}_{\{x:u(x)>\mu\}}(x)\right)$$

is a global minimizer of the P. C. Mumford-Shah model for a.e. $\mu \in (0,1)$.

$\Rightarrow$ UPSHOT: For fixed c_1, c_2, the inner minimization is convex.
$\Rightarrow$ Local minima due to geometry are eliminated.

Generalization to P. C. Mumford-Shah

Generalization to P. C. Mumford-Shah

Generalization to P. C. Mumford-Shah

Stationary state reached

Alternative Methods

- Graph cuts:
  - Anisotropy in the perimeter term.
  - Have to increase connectivity (# of edges per vertex) to converge to isotropic perimeter:

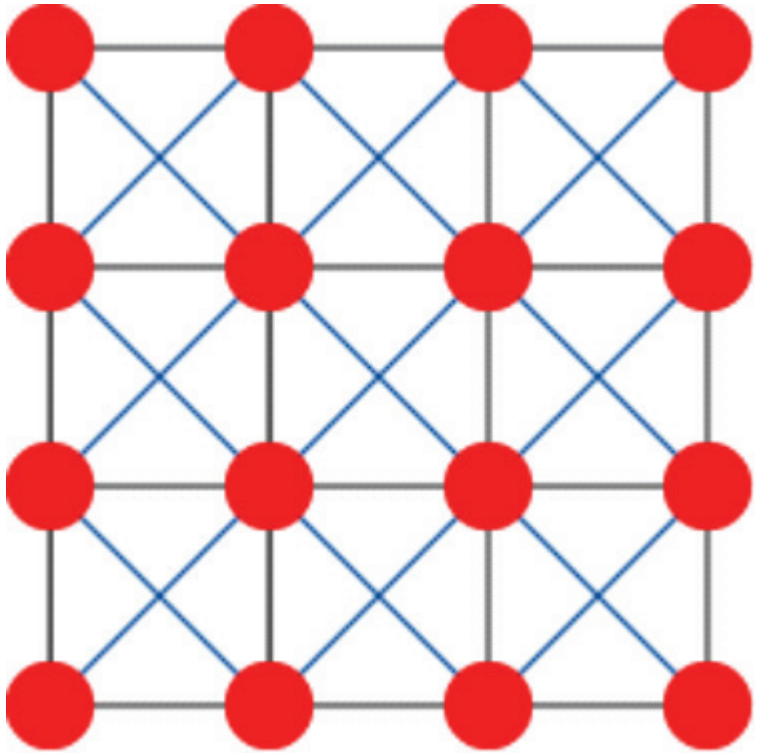

Alternative Methods

- On the other hand, Lucier et. al. show the following:
- Limit of the discrete energies:

$$\sum_{i,j} h^2 \sqrt{\left(D_x^+ u_{i,j}\right)^2 + \left(D_y^+ u_{i,j}\right)^2}$$

as grid size $h \to 0$ is

$$\int |\nabla u|$$

i.e. the isotropic perimeter.

- UPSHOT: With the PDE approach, no need to increase "connectivity" to converge to isotropic shape optimization problem, even though solutions are characteristic functions.

Geodesic Active Contours

- Gradient descent for:

$$\int_0^1 \frac{1}{1 + |(\nabla G_\sigma * f)(\gamma)|^2} |\gamma'(s)| \, ds$$

- Let

$$g(x) = \frac{1}{1 + |(\nabla G_\sigma * f)(\gamma)|^2}$$

- Cohen & Kimmel:
  - Pick two points on the boundary: p & q.
  - Construct the distance function $d_p(x)$ to p.

$$|\nabla d_p| = g(x).$$

  - Gradient descent on $d_p(x)$, starting from q.

Geodesic Active Contours

- Cohen & Kimmel: Unfortunately, no generalization to higher dims.
- Our formulation:

$$\min_{0 \le u \le 1} \int g(x)|\nabla u| + \lambda \int \{(f - c_2)^2 - (f - c_1)^2\}\, u \;\; dx$$

or

$$\min_{\substack{0 \le u \le 1 \\ u(x)=1 \;\forall x \in D}} \int g(x)|\nabla u|$$

- Directly generalizes to any dimension.

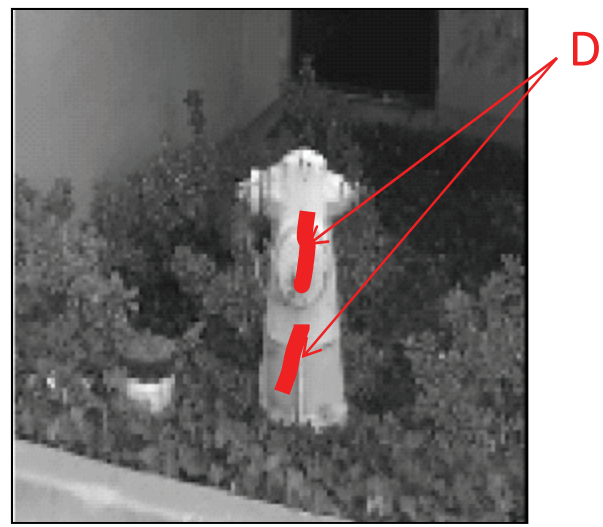

Extensions to Multiphase Setting

- An extension due to Chambolle:

$$\min_{u(x)\in\{c_1,\ldots,c_k\}\ \forall x} \int |\nabla u| + (f-u)^2\, dx$$

- Segmentation into k regions.
- Boundaries weighted very unequally:
  - Let $w_{i,j}$= Weight of interface between Σ_i and Σ_j.
  - Then:

$$w_{i,j} = w_{i,\ell} + w_{\ell,j}$$

where $i > \ell > j$.

Fast TV Iteration

- Chambolle's iteration:

$$p^{n+1} = \frac{p^n + (\delta t)\left\{\nabla(\nabla \cdot p^n) - \frac{1}{\lambda}\nabla f\right\}}{1 + (\delta t)\left|\nabla(\nabla \cdot p^n) - \frac{1}{\lambda}\nabla f\right|}.$$

- Converges for $\delta t \leq \frac{1}{8}$. In practice, can take $\delta t \leq \frac{1}{4}$.
- No dependence on a regularization parameter ε.
- Complexity still $O(N^2)$, where N=Number of pixels (2D).

Fast TV Iteration

- Observe: Chambolle's iteration is equivalent to

$$\frac{p^{n+1} - p^n}{\delta t} = \nabla(\nabla \cdot p^n) - \frac{1}{\lambda}\nabla f - \left|\nabla(\nabla \cdot p^n) - \frac{1}{\lambda}\nabla f\right| p^{n+1}$$

- Explicit time stepping, except for diagonal terms.
- This is the reason for $O(N^2)$ scaling.

Fast TV Iteration

- **Our approach:** Implicit schemes for Chambolle's Euler-Lagrange equation.
- First, consider:

$$\frac{p^{n+1} - p^n}{\delta t} = \nabla(\nabla \cdot p^{n+1}) - \frac{1}{\lambda}\nabla f - \left|\nabla(\nabla \cdot p^n) - \frac{1}{\lambda}\nabla f\right| p^{n+1}.$$

- This is a semi-implicit scheme (implicit off-diagonal terms).
- Unconditionally stable (proof in progress).

Fast TV Iteration

- Let's write out the components:

$$\frac{p_1^{n+1} - p_1^n}{\delta t} = D_{xx} p_1^{n+1} + D_{xy} p_2^{n+1} - \frac{1}{\lambda} f_x - |\nabla(\nabla \cdot p^n) - \frac{1}{\lambda} \nabla f| p_1^{n+1},$$

$$\frac{p_2^{n+1} - p_2^n}{\delta t} = D_{yy} p_2^{n+1} + D_{xy} p_1^{n+1} - \frac{1}{\lambda} f_y - |\nabla(\nabla \cdot p^n) - \frac{1}{\lambda} \nabla f| p_2^{n+1}.$$

- Observe:
  - Only x derivatives on p_1 in the first equation, and
  - Only y derivatives on p_2 in the second equation.

Fast TV Iteration

- Consider: A slightly less implicit scheme:

$$\frac{p_1^{n+1} - p_1^n}{\delta t} = D_{xx} p_1^{n+1} + D_{xy} p_2^n - \frac{1}{\lambda} f_x - |\nabla(\nabla \cdot p^n) - \frac{1}{\lambda} \nabla f| p_1^{n+1},$$
$$\frac{p_2^{n+1} - p_2^n}{\delta t} = D_{yy} p_2^{n+1} + D_{xy} p_1^n - \frac{1}{\lambda} f_y - |\nabla(\nabla \cdot p^n) - \frac{1}{\lambda} \nabla f| p_2^{n+1}.$$

- A great discretization: Solve independent tridiagonal systems.
- Unfortunately: Not unconditionally stable.

Fast TV Iteration

- Stabilization:

$$\frac{p_1^{n+1} - p_1^n}{\delta t} = D_{xx} p_1^{n+1} + D_{xy} p_2^n - \frac{1}{\lambda} f_x - |\nabla(\nabla \cdot p^n) - \frac{1}{\lambda} \nabla f| p_1^{n+1}$$
$$+ D_{yy} p_1^{n+1} - D_{yy} p_1^n,$$
$$\frac{p_2^{n+1} - p_2^n}{\delta t} = D_{yy} p_2^{n+1} + D_{xy} p_1^n - \frac{1}{\lambda} f_y - |\nabla(\nabla \cdot p^n) - \frac{1}{\lambda} \nabla f| p_2^{n+1}$$
$$+ D_{xx} p_2^{n+1} - D_{xx} p_2^n.$$

- Empirical evidence: Unconditionally stable (proof in progress).

Fast TV Iteration

- At every iteration, need to solve

$$\Delta p_1^{n+1} - a(x) p_1^{n+1} = RHS_1,$$
$$\Delta p_2^{n+1} - b(x) p_2^{n+1} = RHS_2.$$

- Independent Poisson equations for p_1 and p_2.
- We solve them by
  - Alternating Direction Implicit (ADI) method,
  - Chebychev acceleration.

Fast TV Iteration

- Slightly faster version:

$$\frac{p_1^{n+1} - p_1^n}{\delta t} = D_{xx} p_1^{n+1} + D_{xy} p_2^n - \frac{1}{\lambda} f_x - |\nabla(\nabla \cdot p^n) - \frac{1}{\lambda} \nabla f|_{p_1^{n+1}}$$
$$+ \theta D_{yy} p_1^{n+1} - \theta D_{yy} p_1^n,$$
$$\frac{p_2^{n+1} - p_2^n}{\delta t} = D_{yy} p_2^{n+1} + D_{xy} p_1^n - \frac{1}{\lambda} f_y - |\nabla(\nabla \cdot p^n) - \frac{1}{\lambda} \nabla f|_{p_2^{n+1}}$$
$$+ \theta D_{xx} p_2^{n+1} - \theta D_{xx} p_2^n.$$

- Empirical observation: Unconditionally stable for $\theta \geq \frac{1}{4}$.
- Every iteration involves:

$$D_{xx} p_1^{n+1} + \theta D_{yy} p_1^{n+1} - a(x) p_1^{n+1} = RHS_1,$$
$$D_{yy} p_2^{n+1} + \theta D_{xx} p_2^{n+1} - b(x) p_2^{n+1} = RHS_2.$$

Fast TV Iteration

Test images:

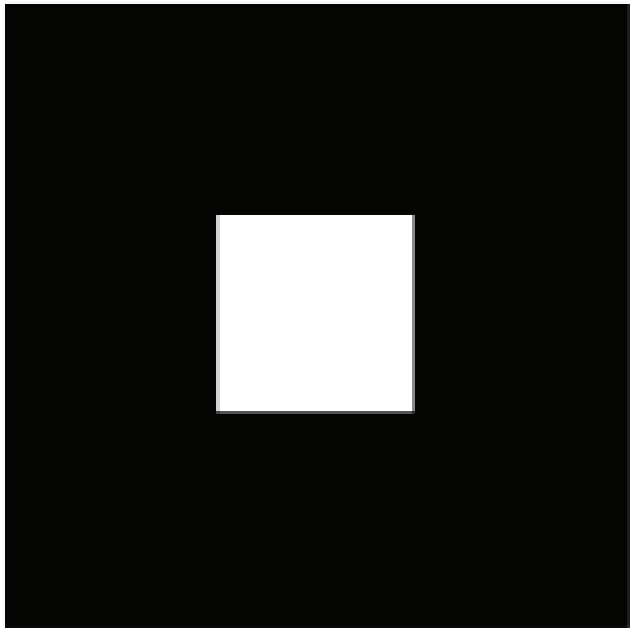

Synthetic Image

Cameraman Image

Fast TV Iteration

- Performance on the synthetic image:

Method	$128^2, \lambda = 0.5$	$256^2, \lambda = 0.5$	$512^2, \lambda = 0.5$
Chambolle	1700; CPU=1	6500; CPU=17	23K; CPU=302
New	8; CPU=0.11	8; CPU=0.5	8; CPU=2.13

- Performance on the synthetic image, bigger λ:

Method	$128^2, \lambda = 1$	$256^2, \lambda = 1$	$512^2, \lambda = 1$
Chambolle	3K; CPU=1.83	12K; CPU=32.8	37K; CPU=458
New	15; CPU=0.22	16; CPU=0.97	15; CPU=4

Fast TV Iteration

- Performance on the cameraman image:

Method	256^2, $\lambda = 0.5$	256^2, $\lambda = 1$	256^2, $\lambda = 2$
Chambolle	5800; CPU=14	17000; CPU=40.7	40000; CPU=96
New	19; CPU=0.74	35; CPU=1.41	70; CPU=2.73

Fast TV Iteration

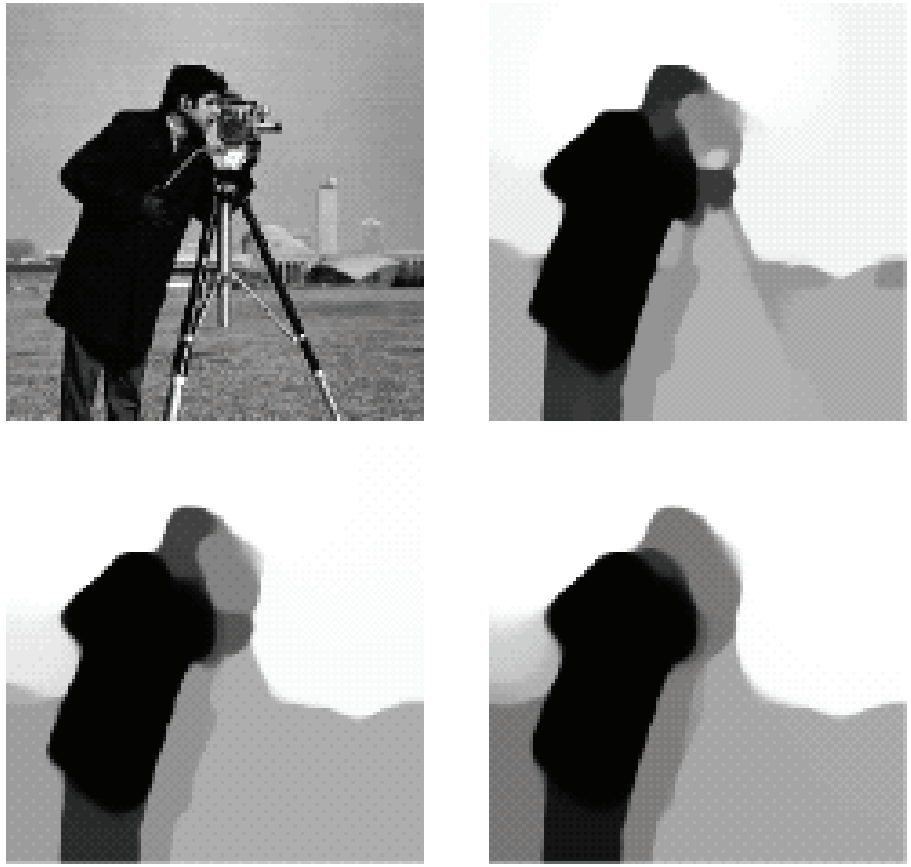

Figure: Original cameraman image, and its processed versions at $\lambda = 0.5$, $\lambda = 1$, and $\lambda = 2$.

Fast TV Iteration

Comparisons with Yin & Zhang's method: Synthetic image at 256^2 resolution, with $\lambda = 0.5$

Residual threshold	Iterations	Error	CPU
10^{-3}	71	11%	2.35 sec
10^{-4}	379	5%	11.6 sec
10^{-5}	4269	1.7%	129 sec
3×10^{-6}	10425	1%	316 sec

New algorithm takes about 0.5 sec.